Low-Temperature Electron and Alpha-Particle Irradiation of Titanium

WALTER BAUER*
Atomics International, Division of North American Rockwell Corporation, Canoga Park, California 91304

AND

K. HERSCHBACH†
Mc Donnell Douglas, Santa Monica, California 90406

AND

J. J. JACKSON‡
Argonne National Laboratory, Argonne, Illinois 60439

(Received 17 March 1969)

The recovery of point defects produced by 1.2-MeV electron and 40-MeV α-particle irradiation has been studied from 50 to 270°K. The recovery spectrum qualitatively resembles that of copper, although shifted to higher temperature. The influence of varying irradiation dose, preirradiation at elevated temperatures, predeformation and dilute alloying were also studied. The recovery below 150°K is dominated by the annihilation of Frenkel pairs, with long-range or uncorrelated migration of the interstitial beginning at approximately 120°K. The recovery of annealed samples irradiated to relatively low dose is characterized by super-recovery. A model involving the migration of interstitial hydrogen impurities from interstitial to substitutional sites is proposed to explain this phenomenon.

I. INTRODUCTION

THE bulk of point-defect studies utilizing charged-particle irradiation at low temperatures has centered on fcc and, more recently, on bcc metals.[1] Relatively little work has been reported in the literature on this type of study on hcp metals. This tendency in interest is virtually inverse to the technological importance of the various metals. While this work on titanium reported here can obviously be justified on its technological merit (low-temperature mobility of defects), it is also of interest from the fundamental point of view (identity and nature of interaction of defects). An additional novel aspect of this work is inherent in the utilization of both 1.2-MeV electron irradiation and 40-MeV α-particle irradiation. This study utilizes techniques for the study of point defects first developed for fcc materials: These include differing irradiation doses,[2] dilute alloying,[2] predeformation,[2] and preirradiation.[3,4]

II. EXPERIMENTAL PROCEDURE

A. Specimen Preparation

Titanium cannot be obtained in high-purity form. The interstitial impurity content of even the highest-purity Ti is rather high. The samples were 5×10^{-3}-in.-diam wire of nominally 99.995% metallic purity, provided by Gallard Schlesinger Chemical Mfg. Corp., Long Island, N. Y. The samples were annealed prior to mounting for 20 min, some 10°C below the α-β transition temperature (~850°C). Since Ti is an excellent getter, the samples were surrounded by Ti foil during the anneal in a vacuum of $\sim10^{-6}$ Torr. Typical resistance ratios ($R_{300°K}/R_{4°K}$) were 17–18; these values were not significantly affected by mounting. However, the ratios were slightly reduced by annealing at temperatures above the transition temperature.

B. Resistivity Measurements

The standard procedure of isochronal recovery measurements involves pulsing a specimen to a given annealing temperature for a fixed period of time and then reading the resistance at a base temperature generally near 4.2°K. This method is capable of accuracies in the range of 10^{-12} Ω cm as long as the resistivity is not a strong function of temperature near the base temperature (Kondo[5] effect), or, if so, excellent temperature control is exercised during the resistance readings. The accuracy of our readings in titanium were unfortunately limited by the Kondo effect.

In earlier work on Ti, Lucasson and Walker[6] reported resistivity increases due to thermal cycling, which they attributed to strain in the grain boundaries. We have found no evidence of this effect after repeated cycling from room temperature to 4.2°K.

C. Irradiation Procedure

The apparatus used for the 40-MeV α-particle irradiation at the 60-in. cyclotron at Argonne has been de-

* Supported by the Metallurgy Branch, Division of Research, U. S. Atomic Energy Commission, under Contract No. AT (04-3)-701. Now at Sandia Laboratories, Livermore, Calif. 94550.
† Supported by the Douglas Independent Research and Development Program.
‡ Supported by the U. S. Atomic Energy Commission.

[1] See, e.g., J. W. Corbett, in *Solid State Physics*, edited by F. Seitz and D. Turnbull (Academic Press Inc., New York, 1966), Suppl. 7.
[2] J. J. Jackson and K. Herschbach, Phys. Rev. **170**, 618 (1968).
[3] J. J. Jackson and K. Herschbach, Phys. Rev. **173**, 664 (1968).
[4] W. Bauer and W. F. Goeppinger, Phys. Rev. **154**, 584 (1967).
[5] J. Kondo, Progr. Theoret. Phys. (Kyoto) **32**, 27 (1964).
[6] P. G. Lucasson and R. M. Walker, Phys. Rev. **127**, 485 (1962).

TABLE I. Experimental results (units of 10^{-8} Ω cm).

		Run	Specimen (annealed) A	Specimen (annealed) B			
			Electron irradiation				
III	ρ_0		259	255			
	$\Delta\rho$		14.5	6.6			
IV	ρ_0		259	255			
	$\Delta\rho$		19.1	10.2			
	$\Delta\rho_{dop}$		0.74				
			α-particle irradiation				
		1	2	3	4	5	6
		Annealed	5.4-at.% Al	Annealed	Deformed	8.5-at.% Al	Deformed
I	ρ_0	325	8450	294	414	18 271	420
	$\Delta\rho$	···	36.7	32.6	···	35.4	27.2
		1	2	3	4	5	6
		Annealed	0.6-at.% Sn	Annealed	Deformed	1.0-at.% Sn	Deformed
IIa	ρ_0	314	1507	296	417	2260	400
	$\Delta\rho$	14.2			11.4		
IIb	$\Delta\rho$		69	71.8		57.7	58.5

scribed elsewhere.[7] Two irradiations with a total of six specimens each were carried out. However, the shutter which permits two specimens to receive a lower dose malfunctioned in run I, so that only four specimens were exposed to the beam. The resultant dose ratios were approximately 1:2.3:5.

The cryostat and associated equipment used in the 1.2-MeV electron irradiations has also been described elsewhere.[8] Here only a pair of specimens was irradiated in each run. A shutter was used to shield one specimen from the higher-temperature preirradiation treatment. Because of the poor thermal conductivity of Ti and the high electron flux required to achieve measurable damage in a reasonable time, the irradiation temperature approached 50°K. Preliminary irradiations with lower fluxes indicated that little recovery occurs between 15 and 50°K.

III. EXPERIMENTAL RESULTS

The geometrical factor required for a conversion of resistance to resistivity is generally not exactly known, since accurate measurements on small specimens are difficult. Here we use the proportionality of the resistance $R_{300°K}$, corrected for residual resistance, to the room-temperature resistivity $\rho_{300°K}$, taken to be 50×10^{-6} Ω cm:

$$\Delta\rho=\Delta R/(R_{300°K}-R_{4.2°K})\times\rho_{300°K}. \quad (1)$$

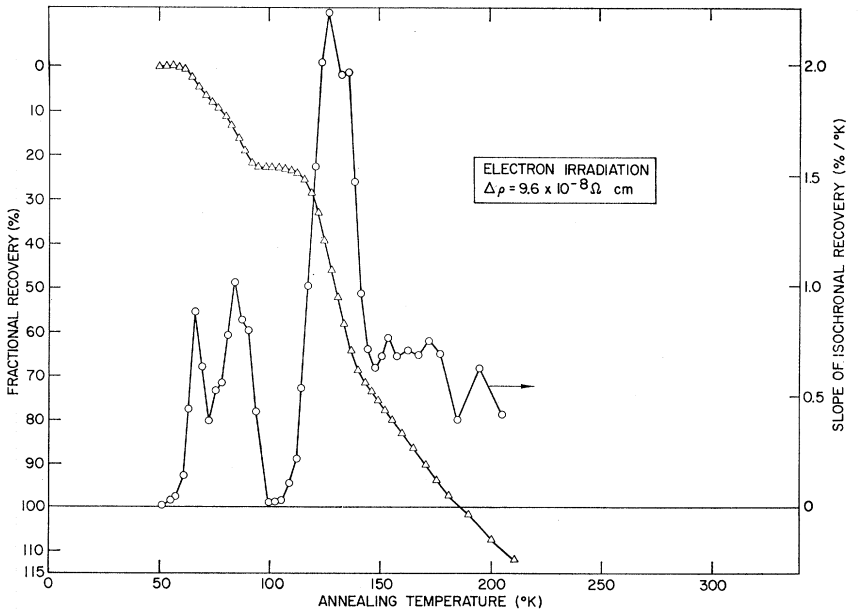

FIG. 1. Fractional recovery and slope of fractional recovery of titanium as a function of temperature after 1.2-MeV electron irradiation (the resistivity increment noted in the figure was calculated without correcting for the residual resistivity and corresponds to sample B of run IV).

[7] K. Herschbach, Rev. Sci. Instr. **37**, 171 (1966).
[8] H. H. Neely, North American Aviation Sr-Memo No. 12404 (unpublished).

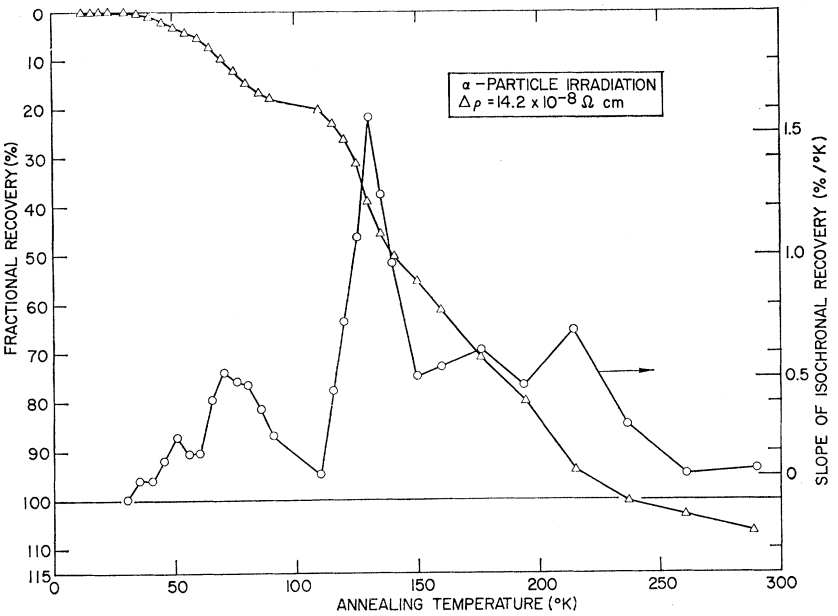

FIG. 2. Fractional recovery and slope of fractional recovery of titanium as a function of temperature after 40-MeV α-particle irradiation.

Because of the high residual resistance $R_{4.2°K}$ of Ti and its alloys and the questionable validity of Matthiessen's rule, this procedure is of limited value. Its main virtue is that it allows a self-consistent comparison of resistivities between the different specimens such as is presented in Table I. Three different doses were employed for the α-particle irradiations shown in Table I as runs IIa, I, and IIb in increasing order of dose. Within each run it is possible to compare the resistivity increment $\Delta\rho$ of pairs of specimens which were essentially behind each other in the beam and thus were exposed to the same particle fluence. The questionable validity of Eq. (1) precludes a quantitative evaluation of the resistivity increment per unit flux $\Delta\rho/\Delta\phi$, but deductions may be made from the relative values of $\Delta\rho$. Prior deformation and alloying with Sn tend to reduce the damage production, whereas alloying with Al tends to increase the damage production relative to the annealed samples.

In Fig. 1, we present the recovery results of specimen B of run IV, 1.2-MeV electron irradiation. Two interesting features are immediately apparent. The first is

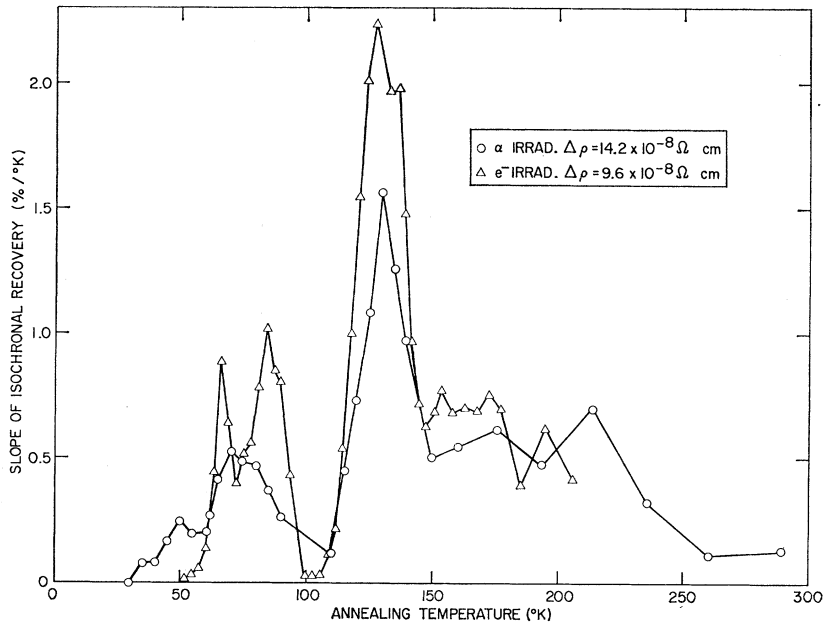

FIG. 3. Slope of fractional recovery as a function of temperature after electron and α-particle irradiation.

that recovery occurs in three well-defined peaks with some unresolved structure on the high-temperature side of the largest of the three peaks. This is quite similar to the recovery spectrum of copper[1]—albeit displaced in temperature. The second is the super-recovery near 185°K. The degree of super-recovery and where it occurs are dependent on the preirradiation state of the sample and irradiation dose. Super-recovery will be discussed in more detail in Sec. IV B.

In Fig. 2, we present the recovery results of specimen 1 of run II, 40-MeV α-particle irradiation. Again, one notes super-recovery occurring at about 240°K. The irradiation temperature during α-particle irradiation was approximately 12°K, substantially lower than during electron irradiation, accounting for the additional recovery below 50°K.

The electron and α-particle irradiations may be compared from the results shown in Fig. 3. Here the slopes of the fractional recoveries after electron and α-particle irradiation are plotted. Below about 180°K there is more recovery and more structure after electron irradiation. In general, there is good agreement in the position of the annealing peaks. The preponderance of low-energy transfers and lack of displacement spikes during electron irradiation tend to create an enhanced and sharper low-temperature recovery spectrum as compared to that after irradiation by heavy charged particles. This is amply evidenced in copper.[1]

We now turn to the recovery studies of samples which have been predeformed at room temperature, alloyed, or preirradiated at 180°K prior to irradiation.

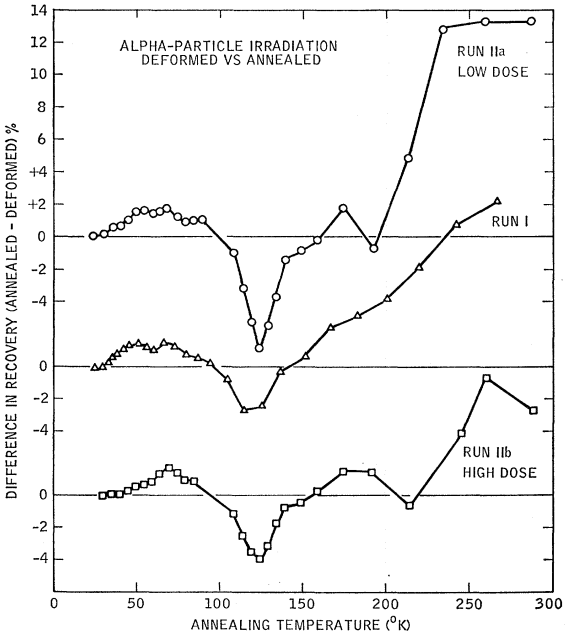

FIG. 4. Difference in fractional recovery of annealed and predeformed samples as a function of temperature after 40-MeV α-particle irradiation. Note the enhanced recovery of the predeformed sample near 120°K.

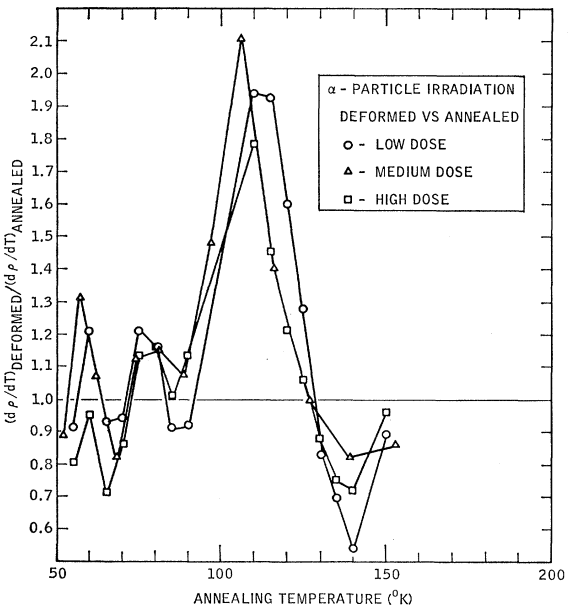

FIG. 5. Ratio of the slope of the fractional recovery of the predeformed to the annealed samples as a function of temperature. Note the enhanced recovery rate of the predeformed samples near 110°K.

The philosophy here is not so much to study the nature of the pretreatment but to use it to gain information about the radiation-produced defects. For example, if a portion of the recovery is due to recombination of close Frenkel pairs, where each interstitial recombines with its vacancy, an excess concentration of vacancies (higher-temperature preirradiation) or excess interstitial traps (alloying) will play a minor role. However, that portion of the recovery associated with long-range defect migration (assumed to be interstitial here) will be affected by pretreatment. In particular, we expect suppression of recovery by alloying (more traps) and enhancement by higher-temperature preirradiation (more vacancies). The effect of deformation is more complex, since both traps (dislocations) and additional vacancies are created if the deformation is carried out at temperatures where vacancies are not mobile.

In order to emphasize the effects of pretreatment on the recovery, we present our data in two forms, both different from the more conventional presentations of Figs. 1–3. Both forms are illustrated for the case of prior deformation. In Fig. 4 we show a plot of the difference in fractional recovery of an annealed and predeformed specimen as a function of temperature, i.e., the curve labeled run IIa represents the difference in fractional recovery of specimens 1 and 4. Clearly, the predeformation enhances recovery starting at ~100°K and reaching a peak near 125°K. A more dramatic way of presenting the same data is via a "serpentine plot" [9] shown in Fig. 5. Here the ratio of the

[9] A. Sosin and K. R. Garr, Bull. Am. Phys. Soc. **10**, 1179 (1965); Phys. Rev. **161**, 664 (1967).

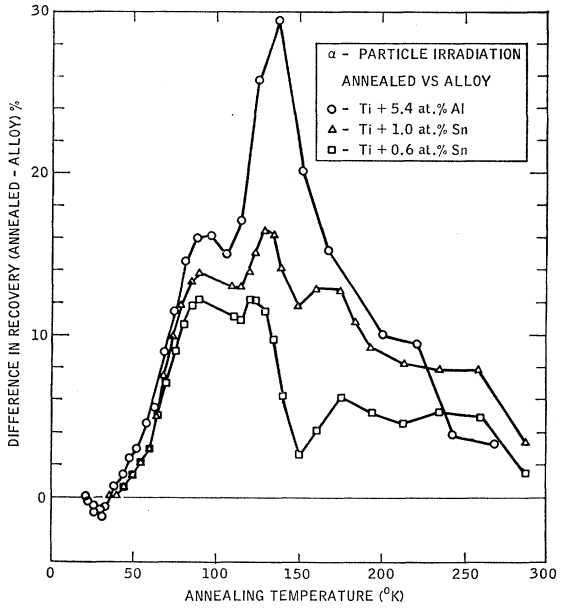

FIG. 6. Difference in fractional recovery of annealed and alloyed samples as a function of temperature.

recovery rates of predeformed and annealed specimens is plotted as a function of temperature. The enhanced recovery near 110°K due to predeformation is emphasized.

The effect of alloying with aluminum and varying amounts of tin on the recovery of titanium is shown in Fig. 6. Here only the differences in recovery between the annealed and alloyed samples are shown. Recovery is suppressed by the addition of the impurities almost throughout the temperature range 50 to ~135°K. Above 135°K the annealed specimen begins to "catch up"; the recoveries of all samples are within a few percent of each other by room temperature. Clearly, the dopants cease to act as traps of radiation-produced defects around 135°K. The connotation "trap" has been used up to now not only to denote the conventional trapping of freely migrating defects, but also to indicate that the recombination of adjacent close Frenkel pairs is inhibited.

We now turn to the effects of varying dose and of preirradiation at 180°K. In Fig. 7, we present the ratio of the recovery rates of samples irradiated to different doses via α-particle irradiation. In each case, a set of annealed and a set of predeformed samples were irradiated to differing doses. If the recovery is governed by the recombination of close Frenkel pairs, we expect very little dose dependence (i.e., the ratios lie near 1 in Fig. 7). On the other hand, if long-range interstitial migration takes place, the ratios should deviate from unity. For the annealed samples the latter seems to be the case near 110°K; close pair recovery dominates below this temperature. On the other hand, the data from the predeformed samples give little indication of serpentine behavior.

In Fig. 8 similar data are shown for electron irradiation. Here the damage ratio is smaller than in the α-particle irradiations, but a small serpentine effect near 140°K is still apparent. This effect is enhanced if sample A is preirradiated at 180°K to the indicated dose $\Delta\rho_{\mathrm{dop}}{}^{A}=(1/37.5)\Delta\rho^{A}$. Because of the super-recovery phenomena in this temperature range, $\Delta\rho_{\mathrm{dop}}{}^{A}$ is unlikely to reflect accurately the concentration of additional sinks.

One set of samples was accidently annealed above the α-β transition temperature prior to electron irradiation. A plot of the data following preirradiation of one specimen according to the format of Fig. 7 gave no indication of serpentine behavior. Also, there was no super-recovery in these samples. Thus their behavior was quite analogous to the predeformed samples of the α-particle irradiation.

IV. DISCUSSION

The main experimental observations which have a direct bearing on any recovery model in Ti are:

(a) "Similarity" of peak structure below 150°K in titanium to that of copper below 60°K.

(b) Super-recovery of annealed samples at relatively low temperature.

(c) Enhancement of recovery rate at ~110°K by predeformation at room temperature.

(d) Suppression of recovery up to 135°K by selected alloying.

(e) Characteristic "serpentine effect" above 110°K upon differing doses of preirradiation.

(f) Suppression of serpentine effect by predeformation or prior annealing above the α-β phase transition temperature.

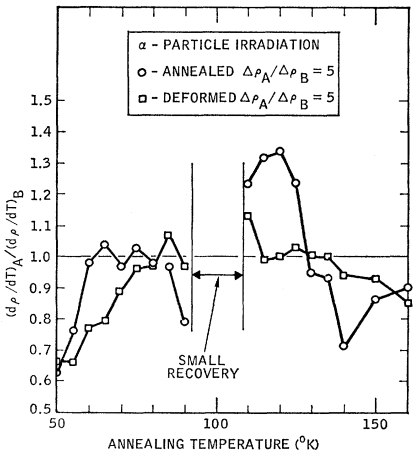

FIG. 7. Ratio of the slope of the fractional recovery as a function of temperature of a pair of annealed and a pair of predeformed samples with samples A and B of each pair irradiated to differing dose.

A. Case of Platinum

We present first some salient results of 2-MeV electron[4] and 20-MeV deuteron[2,3] irradiations of platinum. These results serve as a measure of comparison between electron and heavier charged-particle irradiations such as used in this work. They also serve to demonstrate the effect of preirradiation treatments in a metal for which the low-temperature recovery processes are comparatively well understood.

The mean energy ($\bar{T}$) and maximum energy (T_m) transfers of both sets of irradiations are shown in Table II. The number and temperature intervals of the annealing substages in platinum appear to be independent of energy transfer within the energy range considered. The ratio of the recovery rates of platinum specimens irradiated to different doses is close to the ratio of doses below 23°K after both electron and deuteron irradiations. Above that temperature, the data follow the characteristic serpentine shape indicative of random migration of a defect.

When the vacancy concentration is enhanced by quenching prior to irradiation, the data follow the characteristic serpentine curve above 23°K. This demonstrates that in platinum an interstitial-type defect is mobile at the end of stage I. Large supersaturations of quenched-in vacancies enhance recovery below 23°K in deuteron- but not in electron-irradiated platinum. This enhancement represents the production of additional close Frenkel pairs near vacancies.

In contrast to titanium, plastic deformation of platinum at room temperature prior to irradiation has little effect on the rate of resistivity increase during deuteron irradiation. After predeformation the recovery substages are broadened by the interaction of Frenkel pairs with dislocation strain fields.[2]

B. Super-recovery

In Table III, we have summarized the fractional recovery at 270°K after α-particle irradiation and varying preirradiation treatments. Apparently super-recovery only occurs in annealed samples and depends quite strongly on irradiation dose, being more for lower dose. After electron irradiation, super-recovery is especially pronounced. Super-recovery has been previously observed after electron irradiation of zirconium.[10] In the latter case it has been found to depend on the presence of oxygen impurities.

TABLE II. Mean energy transfer to displaced atom.

Material	Irradiation	Maximum energy T_m (eV)	Threshold displacement energy Td (eV)	Mean energy $\bar{T}$ (eV)
Ti	40-MeV α particle	11.4×10^6	29	374
Pt	20-MeV deuteron	0.8×10^6	36	360
Pt	2-MeV electron	66	36	45
Ti	1.2-MeV electron	120	29	45

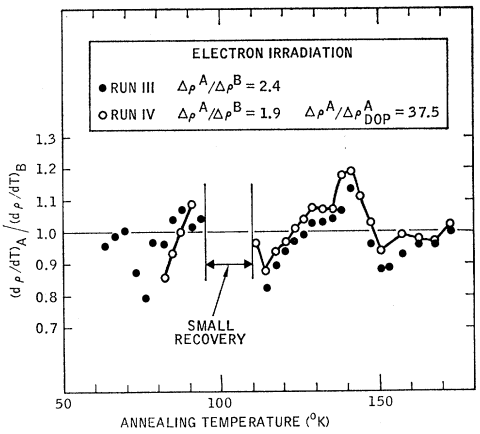

FIG. 8. Ratio of the slope of the fractional recovery of two pairs of annealed samples. In one case samples A and B are irradiated to differing dose; in the other case sample A is also preirradiated at 180°K.

It is very likely that in titanium, because of its phenomenal "gettering" ability, considerable concentrations of oxygen and hydrogen are present.

During long-range migration of the interstitial atoms not all interstitials annihilate at vacancies; some are trapped at impurities or form immobile clusters. Let the concentration of surviving interstitials be C_R and specific resistivity be $\rho_i{}^t$. At a slightly higher temperature range some of the interstitial gaseous impurity atoms (most likely hydrogen[11]) will become mobile and assume substitutional positions at the remaining vacancy sites. Let C_I' and $\rho_I{}^{\text{sub}}$ be the concentration and specific resistivity of substitutional impurity atoms, and C_I and $\rho_I{}^{\text{int}}$ be the initial concentration and specific resistivity of interstitial impurity atoms. Then the condition for super-recovery may be written

$$C_R\rho_i{}^t+(C_R-C_I')\rho_v+(C_I-C_I')\rho_I{}^{\text{int}}+C_I'\rho_I{}^{\text{sub}}<C_I\rho_I{}^{\text{int}}, \quad (2)$$

where ρ_v is the vacancy specific resistivity. Equation

TABLE III. Recovery at 270°K α-particle irradiation.

Run	Specimen	Recovery (%)
I	2,5.4-at.% Al	97
	3, annealed	101
	6, deformed	90.5
II	1, annealed	104.5
	2, 0.6-at.% Sn	92.0
	3, annealed	97.5
	4, deformed	91
	5, 1-at.% Sn	88
	6, deformed	88

[10] H. H. Neely, Bull. Am. Phys. Soc. 13, 1649 (1968).
[11] T. P. Papazoglon and M. T. Hepworth, Trans. AIME 242, 682 (1968).

(2) may be simplified to

$$(C_R/C_I')\rho_i{}^t+(C_R/C_I'-1)\rho_v \overset{?}{<} \rho_I{}^{\text{int}}-\rho_I{}^{\text{sub}}. \quad (3)$$

Two simple cases corresponding to conditional and no super-recovery can be qualitatively evaluated for the cases $C_R/C_I'=1, >1$, respectively. The first case corresponds to low-irradiation dose and Eq. (3) reduces to

$$\rho_i{}^t \overset{?}{<} \rho_I{}^{\text{int}}-\rho_I{}^{\text{sub}}. \quad (4)$$

There are at present insufficient data on specific resistivities to determine whether Eq. (4) is valid. Therefore, super-recovery cannot be ruled out for this case.

The second case, for $C_R/C_I'>1$, corresponds to high-irradiation dose or small number of interstitial impurities. The latter is probably the case for predeformed samples, where C_I' is reduced by precipitation. Equation (3) reduces to

$$(C_R/C_I')(\rho_i{}^t+\rho_v) \overset{?}{<} \rho_I{}^{\text{int}}-\rho_I{}^{\text{sub}}. \quad (5)$$

This inequality clearly does not hold. Consequently, super-recovery is unlikely.

Another possible mechanism for super-recovery involves the precipitation of interstitial impurities at trapped interstitials which remain after the post-irradiation anneal. If all impurities precipitate, the condition for super-recovery is

$$C_I\rho_I{}^{\text{int}}-C_P\rho_P \overset{?}{>} (\rho_i{}^t+\rho_v)-C_P\rho_i{}^t. \quad (6)$$

Here C_P and ρ_P are the concentration and specific resistivity of the clusters, respectively. If the impurities precipitate in few clusters of low specific resistivity, Eq. (6) could be satisfied. Again insufficient data exist on specific resistivities to draw any quantitative conclusions.

C. Recovery Model

The bulk of the data can best be explained by attributing most of the recovery below 150°K to the recombination of Frenkel pairs with long-range interstitial migration starting at 120°K. Above 150°K the recovery mechanisms are complex. Within this model, observations (d) and (e) can be accommodated without any further assumptions. However, some further discussion is required on observations (c) and (f). Here we draw on the discussion of Sec. III A. Deformation clearly results in the production, not only of dislocations, but also of interstitials and vacancies. At room temperature only vacancies and dislocations remain according to our model. Thus observation (c) can be attributed to the additional vacancies present during interstitial migration. Presumably, aging after deformation at a temperature where vacancies are mobile would reduce the effect drastically. Observation (f) can also be explained by the additional vacancies due to predeformation. These vacancies compete with those due to the varying irradiation dose, thus reducing the serpentine effect. A complication enters here due to the fact that this suppression is also observed after heating above the α-β phase transition temperature. Apparently the abrupt cooling results in additional dislocations and vacancies. This would place a rather high limit on the temperature where vacancies are mobile in titanium. Clearly, further work is needed in this area before these tentative suggestions can be adopted.

Broadening of individual recovery peaks due to predeformation as discussed above may also play a role in the interpretation of the serpentine effect. This may be especially pronounced if one of the broadened peaks extends into a temperature range where little recovery occurs in an annealed sample. Clearly, this effect is to be interpreted in terms of long-range interstitial migration.

Two other observations arise when our data are compared with analogous results in platinum. The first is that the height of the serpentine plot in titanium ($\sim$1.2–1.3) in both electron and α-particle irradiation is much lower than in platinum ($\sim$2). The second involves the temperature at which this serpentine peak occurs. In titanium, after electron irradiation, this temperature is $\sim$140 versus $\sim$120°K after α-particle irradiation. In platinum the peak temperature after electron and deuteron irradiation are in good agreement. These differences may be due to different defect configurations or distributions. In any case more work needs to be done before our level of understanding of point defects in titanium is on par with that in platinum.